ARTICLE IN PRESS

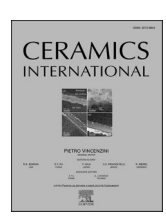
Ceramics International xxx (xxxx) xxx

ELSEVIER

Contents lists available at ScienceDirect

Ceramics International

journal homepage: www.elsevier.com/locate/ceramint



Removing roadblocks and opening new opportunities for MXenes

Michel W. Barsoum a,*, Yury Gogotsi a,b,**

- a Department of Materials Science and Engineering, Drexel University, Philadelphia, PA, 19104, United States
- ^b A.J. Drexel Nanomaterials Institute, Drexel University, Philadelphia, PA 19104, United States

ARTICLE INFO

Keywords:
MXenes
Synthesis
Conductivity
Environmental stability

ABSTRACT

The 2D carbides and nitrides, known as MXenes, are among the most recent, and quickly expanding, material families. The field is experiencing very fast growth with the number of papers on MXenes roughly doubling every year since their discovery in 2011. Great progress in synthesis and control of MXene properties has since been achieved. Synthesis of numerous theoretically predicted MXenes, including ordered solid solutions and highentropy structures, led to the exploration of numerous applications. MXenes are not only promising candidates for energy storage and related electrochemical applications, such as electrocatalysis, but also applications in optoelectronics, plasmonics, electromagnetic interference shielding, medicine, sensing, catalysis and water desalination. We particularly focus on key material manufacturing and stability issues. We describe the scalable synthesis of MXenes by selective etching in aqueous acidic solutions; alternative synthesis methods, particularly fluorine-free synthesis; delamination without the use of organic intercalants; and improving the environmentally stability and shelf life of MXenes in colloidal suspensions. Finally, we discuss the current understanding of electronic transport in MXene films, which is of critical importance for many MXene applications.

1. Introduction

Nanoscale materials or "nanomaterials" have attracted significant attention in the past years. Zero-dimensional (0D) fullerenes, semiconducting quantum dots and metal nanoparticles, as well as onedimensional (1D) nanowires and carbon nanotubes started the nanomaterials revolution towards the end of the last century. In the past decade, we observed a shift from traditional bulk materials production and device manufacturing by subtractive processes to additive manufacturing (3D printing) and self-assembly from nanoparticles. Controlled assembly of nanoparticles results in materials with the required combinations of properties. And a large role in shaping the future material technology belongs to two-dimensional (2D) materials [1,2]. Separation of graphene layers and the discovery of the fascinating physical properties of single- and few-layer graphene in 2004 attracted attention to other 2D materials. Boron nitride, transition metal dichalcogenides and oxides/hydroxides were produced as 2D materials from widely available layered van der Waals bonded precursors. Moreover, new materials that don't have weakly bonded layered precursors, such as silicene, germanene, stanene, phosphorene, borophene and others have been synthesized [3-8].

Among such materials, 2D carbides and nitrides of early transition metals, known as MXenes [9,10], form potentially the largest family, with dozens of well-defined stoichiometric structures, but also a virtually infinite number of solid solutions, some of which are ordered, as well as high-entropy structures. Fine tuning of properties is possible by forming those "2D alloys". The electronic properties of 2D materials range from metallic to semiconducting to insulating. Subnanometer thickness not only leads to mechanical flexibility and optical transparency in 2D materials, but also enables quantum effects due to electronic confinement within atomically thin layers. They also possess quite high theoretical surface areas that are available for adsorption, catalysis and redox processes used in energy conversion and storage. Unlike other nanoparticles, 2D materials can be assembled into dense and strong heterostructures by using flat layers as building blocks. While graphene attracted much attention in the past 15 years, the world is moving from exploiting a single "wonder material" to utilization of potentially hundreds of 2D building blocks with rich chemistries tothat can be assembled for future advanced technologies and applications [3–8].

MXenes have precise 2D structures described by the formula $M_{n+1}X_nT_x$ (M: early transition metal, X: carbon or/and nitrogen, n=1–4) and a variety of surface terminations (T_x is O, OH, halogens,

https://doi.org/10.1016/j.ceramint.2022.10.051

Available online 5 October 2022 0272-8842/© 2022 Elsevier Ltd and Techna Group S.r.l. All rights reserved.

 $^{^{\}ast}$ Corresponding author.

^{**} Corresponding author. Department of Materials Science and Engineering, Drexel University, Philadelphia, PA, 19104, United States. E-mail addresses: barsoumw@drexel.edu (M.W. Barsoum), gogotsi@drexel.edu (Y. Gogotsi).

chalcogens or their mixtures). MXenes come in multiple forms: single element structures ($Ti_3C_2T_x$, Ti_2CT_x , V_2CT_x , etc.), out-of-plane ordered double transition metal o-MXenes ($Mo_2Ti_2C_3T_x$, $Mo_2TiC_2T_x$, $Cr_2TiC_2T_x$, etc.), solid-solution MXenes ($Ti_{2-x}V_xCT_x$, $Mo_{4-x}V_xC_3T_x$, $Ti_{2-x}Nb_xCT_x$, etc.), and in-plane ordered i-MXenes ($Mo_{1.33}CT_x$, $W_{1.33}CT_x$, etc.) [12]. The MXene family is quite diverse, with the materials being tunable through a variety of approaches, including modification of the number of atomic layers (n), changing the M or X elements, adjusting the surface chemistry (T_x) through post-treatment or during synthesis, intercalation of different species into the structure, among multiple other approaches [13–16].

The variety of MXene structures and compositions leads to an enormous variety and wide tunability of properties. For example, the work function of MXenes is tunable from ~ 2 to ~ 6 eV that allows control of junctions in optoelectronics and solar cells. A combination of conductivity with redox ability allows energy storage. Catalytic transition metals in the MXene structures enable electrocatalytic and catalytic applications. Conductivity and transparency of MXenes produces transparent conductors for optoelectronic applications. Tunable plasmon resonance combined with biocompatibility allows MXenes to outperform gold in photothermal therapy and theranostic applications. This list can be continued as MXenes have already found use in multiple diverse fields, and we refer readers to recent review articles for a long list of potential applications of MXenes [15].

To enable industrial scale manufacturing and wide commercial use of MXenes, the research community needs to find a way to overcome a number of obstacles. In late 2020, a group of MXene experts, including the authors of this article, Q. Huang, P. Simon, B. Anasori, M. Naguib, P. Eklund, P. Persson, and J. Rosen with their students and post-docs assembled a list of open questions in the field, which can be found in Ref. [11]. Near the top of the list was research and development efforts directed towards low-cost, scalable, safe, and environmentally friendly synthesis of MXenes with the required compositions, structures and properties. Achieving controlled surface functionalization that would allow further tuning of properties. Increasing environmental stability, shelf and service life of MXenes represent critical challenges. Improving our understanding of key properties, such as the mechanisms of charge transport in single flakes and multilayer MXene films or interactions of MXenes and electromagnetic waves in a broad range of wavelengths, remain important research targets.

The objective of this article is to address a few of the challenges that MXenes, as a still young family of materials, face, describe the state-of-the art in the field and outline some future research directions. We particularly focus on key material manufacturing and storage issues. We describe the scalable synthesis of MXenes by selective etching in aqueous acidic solutions; alternative synthesis methods, particularly fluorine-free synthesis; delamination without the use of organic intercalants; and improving the environmentally stability and shelf life of MXenes in colloidal suspensions. Finally, we discuss the current understanding of electronic transport in MXene films, which is of critical importance for a majority of MXene applications.

2. MXenes produced by wet chemical etching of MAX phases in acidic fluoride solutions

These conductive, hydrophilic 2D ceramics are currently produced via a top-down selective synthesis approach using containers which are resistance to corrosive acids, such as HF and HCl (Fig. 2a and b). Typically, $M_{n+1}AX_n$ MAX phases [17] are used as precursor materials, but some MXenes are synthesized from different precursors, including M_2A_2X and $M_{n+1}Al_xC_{n+x}$ layered carbides. In these cases, A is primarily Al, but Si- and Ga-containing carbides have also been used [12]. MXenes are typically produced in two forms, multilayer, ML, powders and delaminated single- or few-layer flakes. To synthesize ML powders, typically fluoride-containing etchants (HF or HF/HCl) are used to selectively remove the A (in most cases Al) layer. To convert the ML

powder into a single-flake colloidal dispersion, an intercalant (LiCl, tetramethylammonium hydroxide (TMAOH), dimethyl sulfoxide (DMSO), etc.) is used [18]. Another approach uses simultaneous etching and delamination with an *in-situ* HF formation (HCl + LiF, NH₄HF₂, etc.) [18–20].

Scaling the production of MXene to industrial quantities has faced significant challenges due to synthesis bottlenecks, whereby only Ti₃C₂T_r (Fig. 2c) is manufactured in fairly large (kg) quantities. However, even relatively exotic o-MXenes can be manufactured in tens of grams per batch in laboratory environments (Fig. 2d), which is already a large amount for any nanomaterial. The ability to scale up MXene synthesis allows for rapid testing in a variety of fields, where large quantities are needed. However, for this to be the case, the properties that render MXenes appealing need to be conserved in large-volume production. The reaction of the precursor with aqueous solution of HF, HF-HCl or LiF-HCl occurs in the whole volume of the reactor; therefore, the process can be readily scaled with reactor volume. We conducted comparative synthesis of Ti₃C₂T_x in two batch sizes, 1 g and 50 g, to determine if larger-volume synthesis affected the resultant structure or composition [21]. Characterization of the morphology and properties of the produced materials showed that both batches, produced in a small lab setup and in a reactor similar to the one shown in Fig. 2a, were essentially identical. This illustrates that MXenes scaling synthesis is possible, making them viable for further scale-up and commercialization. It is important to note that, while this study showed no difference in structural properties between 1 g and 50 g batch sizes, this does not mean that there will be no technical challenges faced when further scaling to pilot plant levels. However, this step is crucial and promising for the scalable synthesis of MXenes. Furthermore, it is possible to produce large volumes of colloidal solutions of single-flake MXene. Because industrial batch sizes will shortly become available, the production cost of MXenes is likely to be significantly reduced, further promoting their use in wider commercial applications. HF and its derivative are inexpensive chemicals, but their handling requires special precautions [22], increasing the cost of the process. The cost of MAX phase precursors and large amounts of water required for washing the reaction products are other major contributors to the cost of MXene manufacturing.

Synthesis of even 50-100 g batches of MXene (Fig. 1c) provides ample opportunity for commercial production of, for example, MXene inks for printing electronic devices [23]. Because MXenes are synthesized via a topochemical process in an aqueous environment, they maintain their hydrophilic nature. Due to this hydrophilicity, they can be processed using conventional solution-based techniques (primarily water-based), including vacuum-assisted filtration, spray-coating, dip-coating, spin-coating, etc. In addition to aqueous solvents, MXenes form stable colloidal dispersions in polar organic solvents, including dimethylformamide (DMF), N-methyl-2-pyrrolidone (NMP), propylene carbonate, and ethanol [24]. A single 100 g batch of Ti₃C₂T_x provides up to 10 L of 10 mg/mL of aqueous or organic MXene ink, which can be used to print >450,000 interdigitated MXene microsupercapacitors with submicrometer thickness on a 1 cm 2 area at a material density of \sim 3 g/cm³. For electromagnetic interference shielding, a 1.5 μ m Ti₃C₂T_x film currently leads to an effectiveness of $\sim \! 50$ dB. This implies that a single batch of MXene produced could cover more than 20 m² [25]. If utilizing an interfacial assembly approach (assuming a single MXene flake density of ~4 g/cm³) to produce single-layer MXene films for transparent electronics, this batch could instead cover \sim 45,000 m² [26].

3. Fluorine-free etching of MAX phases

If there is a Holy Grail in MXene research it would be to find an aqueous, scalable method to etch the MAX phases without the use of hydrofluoric acid, HF. There are a handful of papers that have claimed to have done so. Close examination of these papers, however, shows that most fall in three categories: i) the evidence for formation of MXenes is

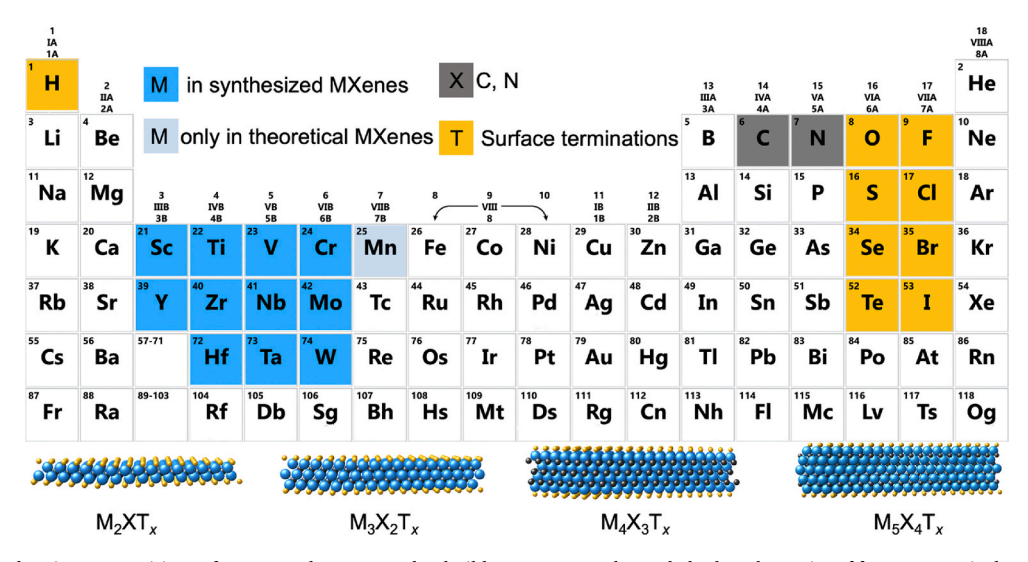


Fig. 1. Periodic table showing compositions of MXenes. Elements used to build MXenes are color-coded. The schematics of four most typical structures of MXenes are presented at the bottom [11]. Copyright ACS, 2021.



Fig. 2. Commercial laboratory scale reactors designed for synthesis of MXene and dried MXene powders after synthesis. (a) MXR204MCW-0.5L reactor (1L and 2L modifications are available at Drexel University); (b) MXR310-1L reactor with an active cooling and heating system and the all-Teflon body; (c) about 70 g of multilayer $T_{13}C_{2}T_{x}$ and (d) about 40 g of $Mo_{2}T_{12}C_{1x}$. (a, b) – courtesy of Materials Research Center, Ukraine. $T_{13}C_{2}T_{x}$ was synthesized by M. Alhabeb and $Mo_{2}T_{12}C_{11}T_{x}$ was made by P. Lelyukh.

weak and/or the work has been difficult to reproduce, ii) The yields are quite low, and iii) the technique does not easily lend itself to large scale production. A brief overview of exploratory work in this field is provided below.

Li et al. heated $T_{i3}AlC_2$ powders in 27.5 M NaOH at 270 °C under an argon atmosphere and claimed to have produced MXene based on XPS spectra and transmission electron microscopy (TEM) analysis [27]. However, the conditions given above are likely to oxidize the MXene sheets formed. We note in passing that the strongest evidence for the formation of MXenes is a C 1s peak of good intensity at 282 eV [28]. Xuan et al. pre-etched $T_{i3}AlC_2$ in HF (which in principle does not make this approach HF free) and subsequently immersed the powders in a tetramethylammonium hydroxide (TMAH) solution to produce MXene [29]. We attempted to reproduce their work, without using the HF step, and ended up with titania-based 2D flakes comprised of 6 \times 10 Ų nanofilaments [30].

Yang et al. [31] reported on the conversion of Ti_3AlC_2 into $Ti_3C_2T_X$ electrochemically using a 1 M NH₄Cl and 0.2 M TMAH electrolyte with a pH > 9, with yields higher than 40%. In this case, there is a 282 eV C 1s peak in the XPS spectra, but also Al peaks, which may come from unreacted Ti_3AlC_2 or from AlO(OH) bonded to the MXene sheets. While removing aluminum oxide/hydroxide may prove difficult, the authors reported large single-layer flakes after delamination. One of us tried but failed to reproduce these results. We thus recommend that others reproduce these results with a sharp eye to the method's scalability and the removal of Al from between the layers. In the work of Sun et al. [32], porous MAX preforms were electrochemically etched in HCl. However, the yields were low, and the process is too slow for commercial purposes. In short, the electrochemical etching may have potential, but much more work, especially with regards to reproducibility and scale-up, is required.

Molten salts etching is a promising technological process [33,34]. At

this time, there is no doubt that the MAX phases can be etched in non-fluorine containing molten salts [33,34]. This approach has the added advantage that, depending on the molten salt used, unary terminations can be obtained [33,34]. When scaling this process, however, one should consider the halide fumes emitted and the large quantities of water needed to wash the excess salt away. It is more difficult to delaminate MXenes made via the molten salt method as compared to those made by wet chemistry methods. No reports on scalable delamination of MXenes produced by etching in molten salts into single-layer flakes are yet available. However, with further research this aspect is probably solvable.

Finally, a room-temperature etching method that utilizes halogens (Br $_2$, I $_2$, ICl, IBr) in anhydrous organic media was recently used to synthesize MXene from Ti $_3$ AlC $_2$ [35]. There is no doubt that other chemical approaches to MXene synthesis will emerge in the future.

4. Delamination protocols for MXenes beyond ${\rm Ti}_3 C_2 T_x$ without the use of organic intercalants

In this realm there is little work. It is generally accepted that to delaminate non-Ti containing MXenes, organic intercalants such as DMSO or TBAOH are required [36-38]. These, in turn, need to be removed if the conductivity of films is to be maximized, adding a layer of complexity to the process that can result in oxidation of the flakes, etc. Quite recently, Natu et al. [39] presented a generalized approach that could be used to delaminate most MXenes without the use of organic intercalants. The main idea, illustrated in Fig. 3, is that by treating HF-etched MXene MLs with NaOH, the Na reacts with the F terminations reducing their concentration. Upon reaction, the F-terminations are replaced by their OH counterparts. Such base-induced dehalogenation is well-established in organic chemistry [40]. Deprotonation of the OH terminations generates protons between the layers that are, in turn, exchanged by Na⁺ ions. The latter bring in water molecules of their hydration shell, expanding the interlayer space and weakening interlayer attraction. At that point, the MLs readily disperse or deflocculate. The XRD pattern of Nb₂CT_x MLs produced by HF etching of Nb₂AlC is shown in Fig. 3b (lower curve blue pattern). When the same MLs were treated with NaCl, there was no change in the patterns (middle red pattern). However, when the same MLs were treated with NaOH (top green pattern), both the intensity and widths of the basal peak, centered around 7° 2θ, increased significantly, evidencing water intercalation.

5. Protecting MXenes from oxidation

MXenes are not stable in water for long times; they oxidize, hydrolize and sometimes totally dissolve. This oxidation is accelerated in the presence of dissolved oxygen [41,42]. Huang and Mochalin [43,44] also showed that water alone can degrade MXenes to methane and metal oxides. As discussed below, this is a serious problem in a host of applications. In what follows we will focus of strategies that have been used to extend the lifetime of, mostly, Ti₃C₂T_x in water. In two of them, the fact that MXenes are believed to oxidize from the edges in, capping agents are used [45,46]. TEM, SEM and AFM studies of MXene flakes and MLs showed the formation of TiO2 nanocrystals along flake edges on initial stage of oxidation. By first showing that the edges of MXene sheets are positively charged and appreciating the fact that the oxidation typically occurs from the edges in, Natu et al. [46] showed that it is possible to greatly reduce the oxidation rates of Ti₃C₂T_x and V₂CT_x MLs by simply adding polyanions - such as polyphosphates, polyborates, and polysilicates - to the colloid suspensions. They then showed by TEM that indeed the polyphosphates – that are the most effective - adsorb on the edges and decrease the oxidation rate of the flakes (Fig. 4). Habib et al. [45] used a similar approach, except they used sodium L-ascorbate as their capping agent. However, long term experiments with capping agents are needed to confirm the effectiveness of this approach. Also, the effect of edge capping on MXene properties films should also be

VahidMohammadi et al. added saturation levels of LiCl and NaCl salts and others to V2CTx suspensions and greatly diminished their propensity for oxidation [42]. They concluded that the cation driven assembly significantly suppresses the oxidation. In light of the work of Natu et al. [46] and Habib et al. [45] an alternate explanation could be the adsorption of Cl at the flake edges. Matthews et al. reported on mild synthesis conditions which result in high-quality V2CTx with fewer defects and an ion exchange process coupled with flocculation that increases the shelf life of this MXene in aqueous suspension by about three orders of magnitude, from a few hours to several months [47]. They also demonstrated that V2CTx produced using ion-exchange to replace tetrabutylammonium or tetramethylammonium ions with lithium cations and flocculation after delamination can not only be stored in suspension for a few months without degradation, but also can be redispersed and processed into films. Those MXene films show distinct improvements in their optical and electronic properties, with the electrical conductivity in the dry state exceeding 1000 S cm⁻¹, a value previously unachievable for V₂CT_r films. The major improvements in shelf life and properties of V₂CT_x should lead to fundamental studies of its properties and expand

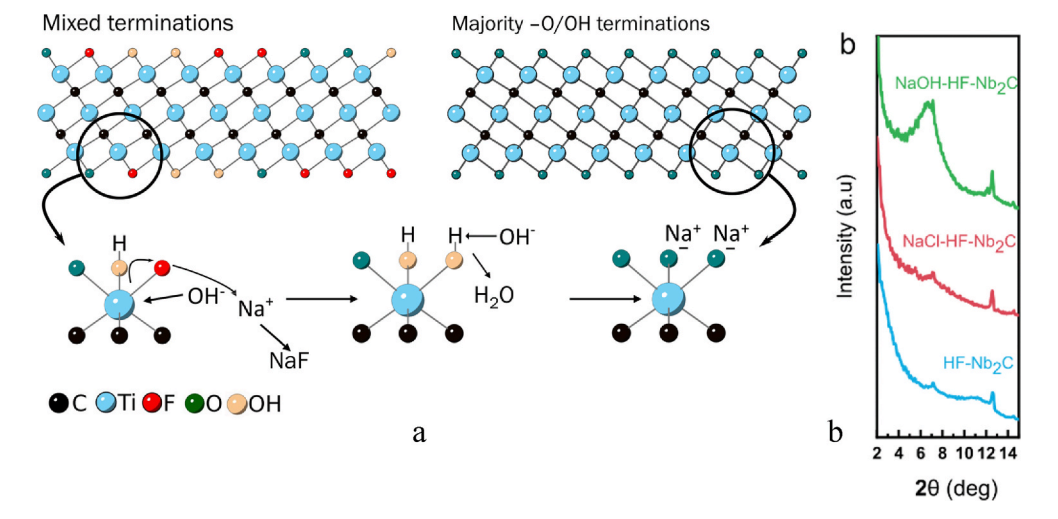


Fig. 3. a) Schematic of process by which F-terminations are replaced by Na cations, that in principle can lead to the delamination of any MXene. b) Low angle XRD patterns comparing effect of treating HF-etched Nb₂CT_x MLs (lower plot) with those washed in NaCl solution (middle) or NaOH (top) [39].

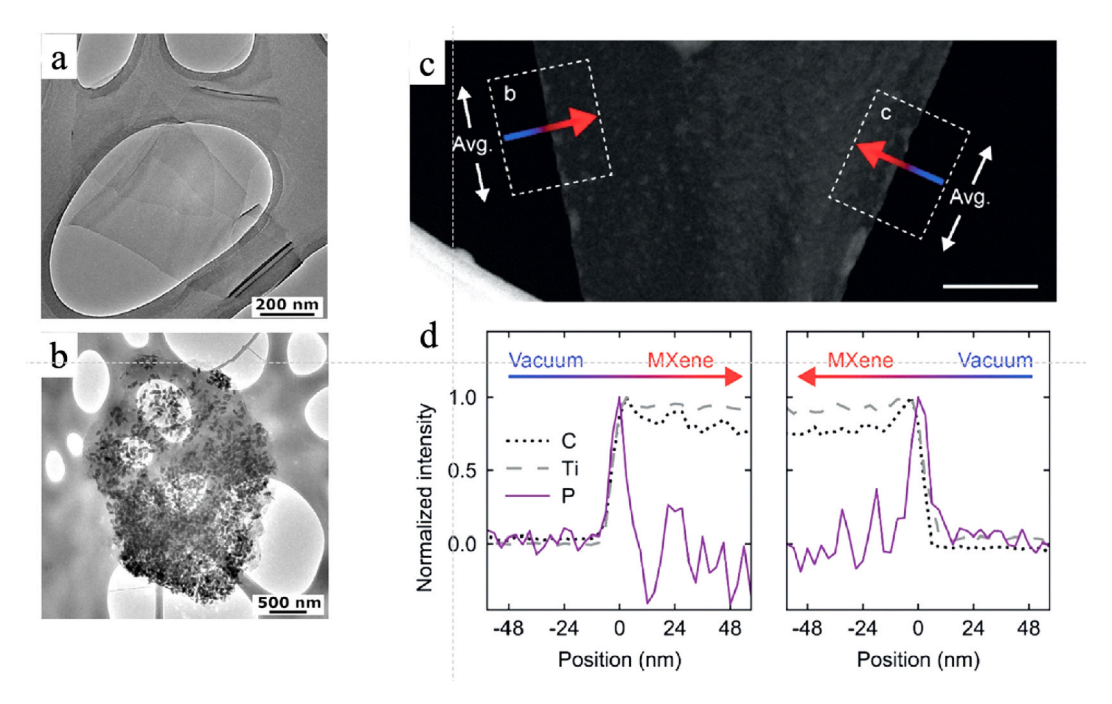


Fig. 4. a) TEM micrograph of a flake treated with polyphosphate and held in an open container for 3 weeks, b) same as (a) but with no polyphosphate; dark spots are TiO₂ particles. c) Same as (a), but now analyzed by EDS along the flake edges; d) EDS results showing concentration of P at the edges only [46].

its range of potential applications. This proposed approach may also be applicable to other MXenes that require the use of quaternary amines for delamination.

Along the same lines, Wang et al. placed ${\rm Ti_3C_2T_x}$ MLs in saturated solutions of cheap, plentiful salts such as NaCl, LiCl, etc. [48] The authors argued that the hydration of these salts decreased the ratio of free water molecules – i.e., water that was not in hydration shells - in solution and showed they reduced the overall concentration of dissolved oxygen, both factors resulting in the protection of MLs. The long-term result, of the order of 12 months, in this study is noteworthy. The downside of this approach is the large quantities of water that would be needed to wash out the salts. In a laboratory setting, for small quantities, this is not an issue, but to scale up to batches that weight multi-kilograms is more of a challenge. In this respect, the use of edge capping is more practical. Before that can be implemented, however, long term experiments with capping agents are needed.

One approach for improving MXene stability under service conditions is to increase their structural perfection and minimize the concentration of defects, including rough edges, where nucleation of oxides starts. Mathis et al. showed that starting with an Al-rich mix when preparing Ti₃AlC₂ precursors one can produce highly stoichiometric Ti₃C₂ with extremely low concentrations of oxygen or vacancies on the carbon sublattice. This resulted in Ti₃C₂T_x flakes that were less prone to oxidation because they contained fewer defects [49]. Produced by this method, delaminated $Ti_3C_2T_x$ remained stable in dilute (~1 mg cm⁻³) deaerated, aqueous colloidal solutions at RT for about a year. Raman spectroscopy and TEM analysis showed no change in the composition and no decoration of single-layer MXene by titania crystals along the edges after 10 months. Other approaches such as freezing MXenes to lower temperatures look less practical, but can probably extend the shelf life of prepared materials by many years [50,51]. Organic solvents can also be used to protect MXenes, as demonstrated for the case of isopropanol [43,44], but solvent transfer and removal of residual water may create an additional challenge. Also, intercalation of organic molecules between MXene layers may affect conductivity and other properties of MXene films.

In this context it is important to note that the aforementioned strategies are only useful for *storing* MXene colloids, including inks for

printing. However, these strategies, for the most part, will *not work in open* systems such as those envisioned during water filtration, desalination, oxidative-based catalysis, etc. This is a serious problem that is *not* being sufficiently addressed by the MXene community. We thus strongly recommend that such experiments be carried out for times commensurate with their projected use time in a given application. Presenting excellent results at short times is important, but, from an application point of view, not of much use. There is currently no good solution to completely prevent oxidation in open aqueous systems or in the presence of oxidizers.

6. Understanding electronic transport in MXene films

Before tackling the question of transport in MXenes it is worth reviewing what is known about the conductivity of the MAX phases [52, 53] as well as very thin layers of MAX phases that were mechanically exfoliated to produce very thin layers of what was termed MAXenes [54]. The metallic character of the conduction of the MAX phase was reported in the first paper on Ti₃SiC₂ [55]. This by itself is not surprising since many early transition metal carbides and nitrides show similar behavior. The explanation was straightforward when Medvedeva et al. showed by DFT calculations that the density-of-states, DOS, at the Fermi level, $E_{\rm F}$, was comprised mostly of d-d orbitals of the Ti atoms [56]. A few years later Hug and Fries showed that the same was true of Ti₂AlN and Ti2AlC [57]. Since then, there are literally tens of DFT and experimental studies that reached the same conclusions. This is important here because this d-d overlap, and the high DOS in MXenes, is inherited from the MAX phases, or, more precisely, from bulk transition metal carbides. One can consider MXene, such as Ti₃C₂, as a (111) slice of a cubic NaCl lattice of TiC. Said otherwise, MXenes are metallic conductors because the binary bulk transition metal carbides and nitrides, as well as the MAX phases, are. In that sense it was not surprising that very thin slivers - half a unit cell thick - mechanically exfoliated MAX phases, or MAXenes, were also metallic conductors [54]. Of course, surface terminations that pull electron density away from the M atoms can affect the DOS at the Fermi level.

It was also quite well-established from the early days that the MAX phases behaved as compensated conductors in that the concentration of

free electrons in the conduction band, n, was roughly equal to that of the holes in the valence band, p. In other words, one needed to worry about, not only n and p, but also their mobilities, μ_e and μ_p . Said otherwise, there are four unknowns n, p, μ_e and μ_p . Between conductivity, Hall voltage and magnetoresistance measurements, one could not solve for all four. However, since these materials appeared to be compensated conductors, then by assuming n=p, or $\mu_e=\mu_p$, one could solve for all four [52]. It was always acknowledged, however, that there was no physical basis for making such an assumption that apparently works for many MAX phases.

The riddle was solved by Ouisse and co-workers, who plotted the Fermi surfaces, FS, of the MAX phases and showed that in many of them they could, as a first and good approximation, be considered to be 2D hexagonal metals [58,59], as illustrated in Fig. 5. Fig. 5a plots the DFT-derived FSs of Ti₂AlC. Fig. 5b compares a projection of the FS on the basal plane (in color) with the 2D Fermi lines assuming a simple *near free electron* 2D hexagonal metal (in red). The excellent agreement between the 2D approach (red lines in Fig. 5b and the more involved DFT-based projections suggests this approach has merit. Fig. 5c, d and e, plot the 2D Fermi lines, velocity moduli and mean free paths of the electronic carriers, respectively [53,58].

In several 2D systems, including graphite, the best interpretation for out-of-plane conductivity is that it is due to interlayer defects. The implications of these conclusions to MXenes is obvious and will not be belabored here; the details can be found in Ref. [53].

Transport in MXene films, σ_{films} , is complicated because it is a convolution of individual flake conductivity, σ_{flake} , and that between flakes, σ_{inter} . If measurements are carried out on single flakes, the

interpretation of σ_{flake} is fairly straightforward. And while the interpretation is straightforward, the measurements are quite tedious indeed. Not only is the possibility of damaging the flakes during preparation of the samples a constant concern, but also their oxidation (see above). As far as we are aware, there are only a handful of studies that have attempted to do so [60-63]. Miranda et al. were the first to report on the electrical characterization of single multi-layer MXene Ti₃C₂T_x flakes [60]. In this case, σ_{flake} was $\approx 900 \pm 300 \text{ S cm}^{-1}$ with $n \approx 8 \pm 3 \times 10^{21}$ cm⁻³; their mobility, at $\approx 0.7 \pm 0.2$ cm² V⁻¹ s⁻¹, was low. Lipatov et al. [62] working with higher quality single-layer Ti₃C₂T_x flakes estimated $\mu_e \approx 2.6 \pm 0.7 \text{ cm}^2 \text{ V}^{-1} \text{ s}^{-1}$ and $n \approx 1 \times 10^{22} \text{ cm}^{-3}$, the latter comparable to that of Miranda et al. The later studies were conducted on stoichiometric high-quality single-layer Ti₃C₂T_x flakes with a Ti:C atomic ratio quite close to the ideal value of 1.5 and improved chemical stability [49]. Those samples exhibited electrical conductivities of up to 11,000 S cm⁻¹ and field effect electron mobilities of up to 6 cm² V⁻¹ s⁻¹ [64], both representing an improvement by a factor of two compared with the values reported in their previous study of similar Ti₃C₂T_x field effect transistors. Those measurement convincingly show that MXene monolayers with fewer defects possess higher electronic conductivities and

In principle, the free carrier numbers are important and should be much more *intrinsic* to a given MXene composition than their mobilities that are affected by defects, etc. This is *only* true, however, when it is established that the single flakes are *not* oxidized. If one assumes the total number of electrons per unit cell populating all partially filled bands is 6, then the n derived from the 2D hexagonal metal model alluded to above, $\approx 10^{22}$ cm⁻³, is in good agreement with the

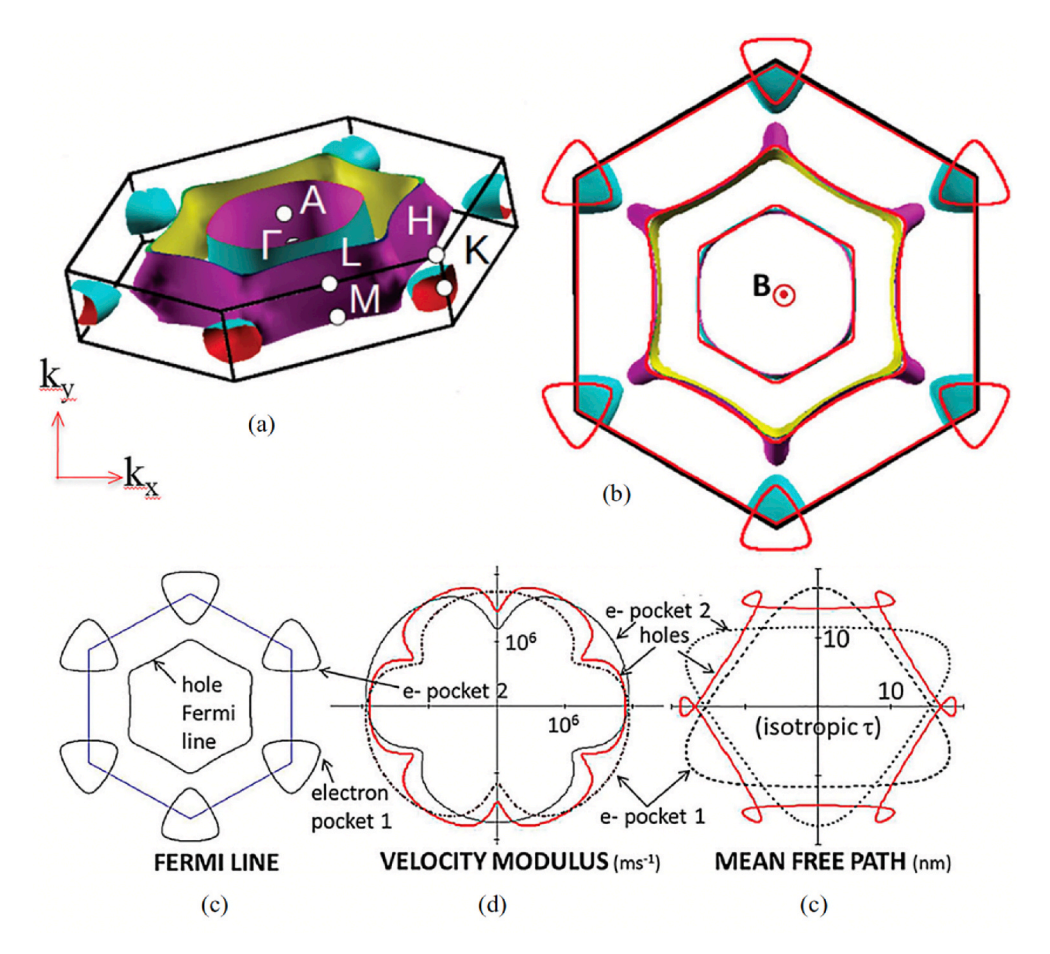


Fig. 5. a) DFT-derived Fermi surface of Ti₂AlC, (b) projection of FS on basal plane (in color) and 2D Fermi lines assuming a simple near 2D electron free model (in red). (c) 2D Fermi lines and corresponding, (d) radial plot of velocity, and (e) mean free paths. Applied magnetic field, B, is into the page. For details see Refs. [53,58].

experimental results.

In the case of single ${\rm Ti_3CNT}_x$ flakes, $\sigma_{\rm flake}\approx 1300\pm 50~{\rm S~cm}^{-1}$ [63]. The mobility was $1.4\pm 0.25~{\rm cm}^2/{\rm V}$ s, for an n of $5.8\times 10^{21}~{\rm [cm}^{-3}$. This value is lower than for ${\rm Ti_3C_2T}_x$ flakes. Interestingly, DFT calculations predict that the carbonitride flakes should have a higher n. In the same paper, the authors carried out Hall measurements on filtered films. In that case, n and μ_e were $\approx 8.2\times 10^{21}~{\rm cm}^3$ and $\approx 0.58~{\rm cm}^2/{\rm V}$ s, respectively.

Lipatov et al. [61] measured the conductivities of single Nb₄C₃T_x flakes and concluded their conductivity was n-type, with $\sigma_{flake}\approx 1000$ \pm 200 S cm $^{-1}$. The mobility was measured to be 0.44 cm 2 V $^{-1}$ s $^{-1}$, rendering $n \approx 1.4 \times 10^{22} \, \text{cm}^{-3}$, which is of the same order of magnitude as for $\text{Ti}_3\text{C}_2\text{T}_x$. Importantly, σ_{flake} values for two layered, 2L, and three layered, 3L, assemblies were higher than the single layered, 1L, ones. For example, at 1800 S cm $^{-1}$, σ_{flake} for 3L was almost double that of 1L. The mobility in the 3L case was 0.7 cm² V⁻¹ s⁻¹, for an $n \approx 1.6 \times 10^{22}$ cm, which is slightly higher than the value obtained in the 1L case. This decrease in conductivity was ascribed to oxidation of the 1L flakes. This in turn brings up a serious concern of single flake measurements: What exactly is being measured, a pristine MXene flake or its partially oxidized counterpart? While the stoichiometric single-layer Ti₃C₂T_v flakes experienced little change for several weeks in our experiments, many other MXenes oxidize much faster. We thus recommend that when such single flake measurements are attempted extreme care be taken in trying to minimize their oxidation. One possible way to do so would be to cap the edges before separating the flakes. Alternatively, measurements should be carried out as a function of the number of layers and then assume that the highest values obtained per flake are closer to the intrinsic value. Preparation and testing in inert environments, such as a glovebox, certainly helps to minimize their oxidation and adsorption of undesired species on their surface.

We now turn our attention to films comprised of overlapping flakes. In this realm we want to make a further distinction between spin-coated films and ones that were simply drop cast or filtered. In the former, the flakes usually align parallel to the substrate and variability between researchers is reduced. The same is not true of filtered films or drop-cast films in which the variables are significantly higher, and the results obtained are much more scattered. We start with work on spin coated films.

The first study on conductive and transparent spin coated $Ti_3C_2T_x$ films was published by Dillon et al. [65] In this case, σ_{film} was 6500 \pm 800 S cm $^{-1}$. Using Hall effect measurements, they concluded that their mobility was ≈ 0.9 cm 2 V $^{-1}$ s $^{-1}$ and $n \approx 3.1 \times 10^{22}$ cm $^{-3}$. Note this n value is ≈ 3 times greater than the results on single flakes reported above. In Ref. [60], the σ_{flake} values were lower than σ_{film} which may result from material oxidation. In two studies on $Ti_3C_2T_x$ by Lipatov et al., the conductivity values measured on single-flakes and multilayer films were similar [62,64]. These facts need explanation. Results on single Nb₄C₃T_x flakes are more robust because in that case σ_{flake} was roughly two orders of magnitude higher than films made of similar flakes [61].

6.1. MXene from epitaxially grown MAX films

In 2014, Halim et al. [20] deposited epitaxial films of Ti₃AlC₂ with their basal planes parallel to a sapphire substrate and etched them using HF or NH₄HF₂. The films were both transparent and conductive. In a sample with a film thickness of 30 nm, dp_{film}/dT was positive down to 100 K, before it became negative. In the low T regime, the results best fit a weak localization model, viz. $R \propto \ln T$. It is important to note that the differences in pfilm for the two films with d values of 1 nm and 12.5 nm were 2.3 and 5 $\mu\Omega$ m, respectively. The sensitivity of these films to d, λ , are thus of the order

$$\lambda = (2.3-5)/(1-1.25) \approx -9.4 \times 10^{14} \text{ S/m}^2$$

Intriguingly, when d was 12.5 nm, $d\rho_{film}/dT$ was close to zero. The importance of this observation is discussed below.

In 2019, Halim et al. [66] deposited Ti_2AIC and Nb_2AIC epitaxial thin films, again on sapphire substrates, by physical vapor deposition. The films were etched in LiF/HCl solutions, yielding Li-intercalated 2D Ti_2CT_x and Nb_2CT_x films. The former exhibits metallic conductivity, with weak localization below 50 K. In contrast, the Nb-based films exhibit an increase in resistivity with decreasing temperature from RT down to 40 K consistent with variable range hopping, VRH, transport.

6.2. Filtered films

The most complicated conductivity is that of films, produced by drop casting or vacuum assisted filtration, VAF, wherein $\sigma_{inter}\ll\sigma_{flake}.$ This is due to wide variations in film densities and flakes' orientation in those films. The implication of this simple inequality is far reaching, the most important being that it is difficult to say anything definitive about σ_{flake} from measurements made on thin films. It is worth repeating that as long as $\sigma_{inter}\ll\sigma_{flake},$ then per *force*, any changes in film transport behavior primarily reflect changes in $\sigma_{inter},$ that may, or may not, be related to changes in $\sigma_{film}.$

We now examine some papers in the literature dealing with $\sigma_{\rm film}$, or their resistivities, $\rho_{\rm film}$. To date, the response of the latter to temperature, T, has been mostly either metal-like, where ${\rm d}\rho_{\rm film}/{\rm d}T$, is positive [20], or ones where ${\rm d}\rho_{\rm film}/{\rm d}T$ is negative [38]. In the former case, there is not much to be discussed except to note that it is unusual for a collection of metallic entities, such as individual MXene flakes, surrounded by thin insulating layers, such as water and/or terminations, to behave in a metal-like fashion. This point is further discussed below.

The magnetotransport of freestanding VAF films of Mo_2CT_{x} , $Mo_{1.33}CT_{x}$, $Mo_{2}TiC_{2}T_{x}$, and $Mo_{2}Ti_{2}C_{3}T_{x}$ was measured in the 10–300 K temperature range [38]. Some of the films were annealed before measuring their transport properties and several studies were combined [38]. Analysis of the resistivity results in the 10–200 K temperature, T, regime (Fig. 6a) suggest—with the exception of the heavily defective $Mo_{1.33}CTx$ composition, variable range hopping, VRH, between individual MXene sheets is the operative conduction mechanism [67]. For $Mo_{1.33}CT_{x}$, because of large defect concentration, it is more likely that VRH within individual flakes is rate limiting. At higher temperatures, a thermally activated process emerges in all cases.

In the VRH mechanism, the hopping is controlled by tunneling across thin insulating layers separating highly metallic islands/grains. The charge carriers are assumed to hop from flake to flake across a distribution of distances assisted by phonons. What gives this approach credibility is that the response of various MXene compositions with T share characteristic features already observed in systems where highly conductive entities are separated by thin disordered regions such as granular metals and cermets as opposed to "homogeneous" amorphous semiconductors [38].

Notably in this work, $\sigma_{\rm film}$ was found to be an exponential function of d (Fig. 6b), but intriguingly not equally. For example, compare ${\rm Ti}_3{\rm C}_2{\rm T}_x$ and ${\rm Mo}_2{\rm CT}_x$. For the ${\rm Mo}_2{\rm CT}_x$ films, increasing d from 0.8 to 1.9 nm, increases the resistivity by almost *five orders* of magnitude [Fig. 6b]. The Mo-Ti films' sensitivity to d is in between those of ${\rm Mo}_2{\rm CT}_x$ and ${\rm Ti}_3{\rm C}_2{\rm T}_x$ with $\lambda \approx$ given above (see red line labelled Ti epit in Fig. 6b). In light of these results, it is reasonable to conclude VRH in Ti-containing films is significantly easier than in non-Ti-containing MXenes. The reason for this state-of-affairs is unknown at this time.

Kim et al. [68] showed that after annealing Mo_2CT_x , $Mo_2TiC_2T_x$ and $Mo_2Ti_2C_3T_x$ samples in Ar/H_2 gas at 800 K, the nature of the conductivity in the former two became metal-like. The same is true in the work of Hart et al. [69] who *in situ* heated $Ti_3C_2T_x$, Ti_3CNT_x and $Mo_2TiC_2T_x$ multilayer films in vacuum of TEM. The observed changes in ρ_{film} were, not surprisingly, due to removal of intercalated molecules, leading to a reduction in d, and due to changes in the nature of the functional groups. In most cases, with the notable exception of the $Ti_3C_2T_x$ films, the initial

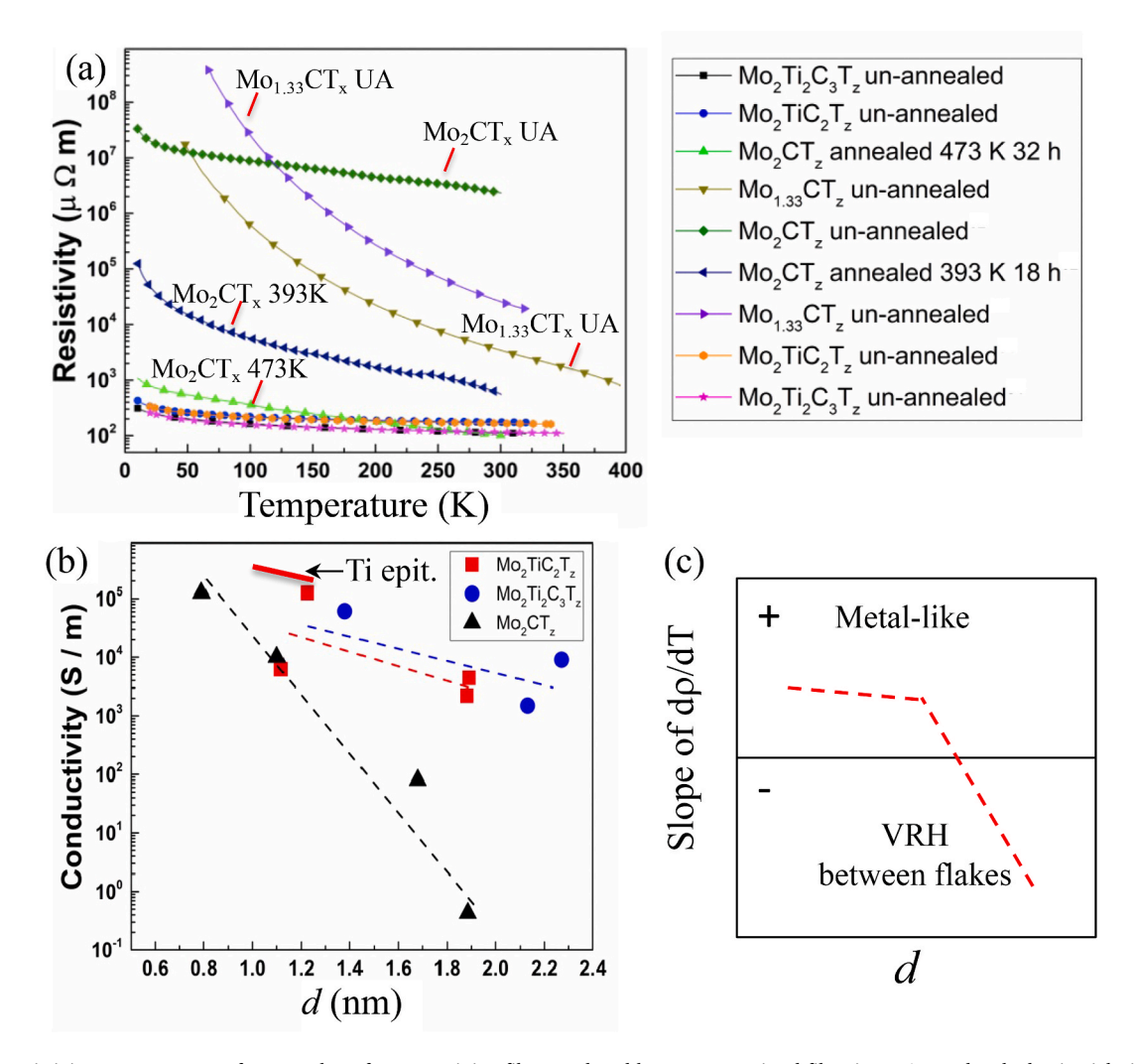


Fig. 6. a) Log resistivity vs. temperature for a number of Mo-containing films produced by vacuum-assisted filtration, VAF. and etched epitaxial Ti_3C_2 films [20]. Panel on right is key to (a) taken from Ref. [38] b) effect of interlayer distance, d, on conductivity [38]; (c) Summary of $d\rho/dT$ vs. d results. At large d, VRH is operative mechanism; at low d, the response is metal-like, where effect of d on resitivity much less dramatic.

response was one where ${\rm d} \rho_{\rm film}/{\rm d}T$ was negative, but as more of the intercalants and surface functionalities were removed at higher temperatures, as confirmed by electron energy loss spectroscopy (EELS) and evolving gas analysis, ${\rm d} \rho_{\rm film}/{\rm d}T$ became positive, i.e., the response became metal-like.

Crucially, these results, and those of others, that have shown the similar responses [63,68,69], are fully consistent with the conjecture that the flakes of those MXenes themselves remain metallic in nature at all times, i.e. the VRH model is applicable. The conclusion that the conductivity was due to VRH was first reached in 2018 by Halim et al. [38], and later adopted by others [63,68,69]. When d is large, $d\rho_{\rm film}/dT$ is negative because we are dealing with VRH. Once d between the flakes gets small enough – by intercalant removal, for example – the true metallic nature of the flakes manifests itself.

From the totality of the results obtained to date, the following tentative proposition can be made: When $d\rho_{\rm film}/dT$ is close to zero [20, 38,69], it is reasonable to assume that the VRH and metallic conductivity are balanced to yield a $\rho_{\rm film}$ that has a very weak dependence on T.

It is worth noting that in the VRH regime Hall data *cannot* be used to estimate electron concentrations, for the simple reason that in most disordered systems it is unlikely that a simple relation connecting the density of states at the Fermi level, $D(E_{\rm F})$, to the total carrier concentration in a band exists [67]. This is an important conclusion that cannot be easily dismissed because it implies that in the VRH regime, DFT

calculations of say $D(E_{\rm F})$ of a given composition *cannot* be used to explain conductivity changes. This, in turn, implies that the individual flake results are much more reliable, assuming no oxidation, compared to Hall results on ${\rm Ti_3CNT}_x$ films [63] whose conductivity remain in the VHR regime.

To summarize this section, refer to Fig. 6c. When d is large, $\mathrm{d}\rho_{\mathrm{film}}/\mathrm{d}T$ is negative and we are dealing with VRH [38]. As d decreases as a result of annealing, for example, $\mathrm{d}\rho_{\mathrm{film}}/\mathrm{d}T$ becomes positive viz. metal-like. In this regime, the effect of d is much less important, and the changes can, with many caveats, be related to $D(E_f)$. At what d, the transition between VRH and metal-like conductivity occurs is sensitive to MXene chemistry. For the most studied MXene, $\mathrm{Ti}_3\mathrm{C}_2\mathrm{T}_x$, the transition occurs at relatively larger d values than say the Mo-based ones. Here we do not mean to imply that d solely determines electronic transport. As noted above, the relationship is complex. For example, the higher the value of n in $\mathrm{M}_{n+1}\mathrm{C}_n\mathrm{T}_x$, the more conductive the films for the same d and the less sensitive the conductivity is to d [Fig. 6b].

Lastly, some have referred to the regime when $d\rho_{film}/dT$ is negative, as a semiconductor-like temperature response [69,70]. However, VRH can occur in highly degenerate semiconductors as well [67]. The analysis of Halim et al. [38] clearly showed that, at least for Mo-based MXenes, this response was not due to the latter. Insufficient experimental data -especially measurements on single-layer flakes, for many other MXenes - makes it difficult to determine if any MXenes,

synthesized to date, show a band gap and semiconducting behavior.

6.3. Terahertz spectroscopy

A powerful technique to decouple σ_{inter} from σ_{flake} is to use terahertz, THz, spectroscopy [71]. This is possible because at THz frequencies the lengths scales, L, probed are given by:

$$L = \sqrt{\frac{D}{\omega}}$$

where D is the carriers' diffusion coefficient. For a typical $D \sim 10$ cm²/Vs and $\omega = 2\pi \times 10$ [12] s⁻¹, $L \approx 13$ nm. In general, the agreement between conductivities obtained using this technique and DC measurements in MXene thin films is good [72,73]. The advantage of this method, however, is that it is contactless. What is well characterized by this technique are scattering times and localization. To convert these values to number of carriers and/or mobilities requires models. Starting with Ti₃C₂T_x films processed using an interfacial thin film technique, Li et al. [73] reported $n \approx 2 \times 10^{21} \text{ cm}^{-3}$, and a μ_e of $\sim 34 \text{ cm}^2 \text{ V}^{-1} \text{ s}^{-1}$. Why *n* is roughly an order of magnitude lower than those measured for single flakes is unclear but is most probably related to the simplicity of the Drude model that assumes the electrons behave isotropically as atoms in a gas phase. It thus follows that until this discrepancy can be understood, the n values obtained from this technique are useful for comparative purposes only. Where this technique is quite useful, however, is in tracking changes in σ_{film} as a function of, say, annealing, temperature, or the nature of the intercalants.

To further advance our understanding of MXenes' electronic properties, synergistic theoretical and experimental efforts are needed. There are numerous theoretical papers in the literature that predict important changes in σ_{flake} as a function of the nature of the terminations. And in many cases these predictions have been used to explain changes in $\sigma_{\rm film}$, as the review of literature shows [74]. One should be cautious, however, because as mentioned several times above, it is not always possible to relate σ_{flake} to σ_{film} , especially when $\sigma_{flake} \gg \sigma_{film}$. When changes in σ_{film} are measured as a function of temperature, it is important to distinguish between two different types of changes: changes in the nature of the terminations and changes in the interlayer distance, d [69]. These changes sometimes occur in series and sometimes simultaneously, further convoluting analysis. It is important to note here we are not advocating that σ_{flake} is not important, but simply that there is no direct connection between σ_{flake} and σ_{film} . One of the advantages of the VRH model is that indeed it takes the DOS at E_F into consideration. What is urgently needed are theoretical models that can model $\sigma_{\text{inter}}.$ Given that this problem has been in the literature for over 60 years, however, implies that the problem is non-trivial. The fundamental problem with understanding transport in ML MXenes is that, apart from the VRH model, there are no good theoretical models that can be tested.

7. Conclusions and outlook

We have shown that MXenes are coming out of age. They are among the few nanomaterials that can be produced in large quantities by a fairly simple selective etching process. Aqueous, and nonaqueous, liquids and molten salt etchants can be used but the synthesis is still to be scaled up to the industrial scale. While significant progress has been achieved in MXenes' development, there are many remaining challenges.

As discussed above, environmentally friendly, safe, efficient, and scalable synthesis methods are being developed, but there is still much work left to do. Most MXenes are built of abundant elements, such as Ti, V, C, N, etc., and can potentially become low-cost materials, but this would require decreasing the cost of synthesis of both, the MAX phase precursors and MXenes. The search for new precursors should continue. Direct synthesis of MXenes from elements, topochemical transformation

of 2D oxides and other methods should be explored as well.

The chemical and temperature stability of $Ti_3C_2T_x$ and V_2CT_x MXenes has been improved, as recent publications show. $Ta_4C_3T_x$, $Nb_4C_3T_x$ and other M_4C_3 structures have demonstrated good environmental stability as well, but improvement in the synthesis and storage processes should be carried out for Ti_2CT_x and many other MXenes that have limited environmental stability, and which prevents their storage and shipping to potential end-users.

In general, further exploration of MXenes beyond ${\rm Ti}_3{\rm C}_2{\rm T}_x$ is needed. High-entropy MXenes may have higher environmental stability, but their exploration just started. Development of o-MXenes with the arrangement of constitutive elements providing the maximum oxidation resistance should be explored. Control of surface chemistry and manufacturing of large single-crystal MXene flakes with minimal edge areas may also improve their environmental stability.

Development of delamination protocols for MXenes beyond Ti_3C_2 without the use of organic intercalants that will provide improved conductivity, oxidation resistance and other properties would be of importance. Development of self-assembly techniques to prepare MXene films with aligned flakes and controlled orientation/distance between flakes may allow utilization of 2D MXenes as nanoscale building blocks for developing 3D nanoarchitectures, including vertically aligned, hybrid and other structures.

Understanding intra- and inter-flake charge transport in single- and ML MXenes is emerging. It is very important for many applications that rely on the conductivity of MXenes. However, studies on single-layer flakes have been performed on only 2 MXenes so far (Ti_3C_2) and Nb₄C₃ and fundamental studies on other MXenes are needed to decouple intraflake transport form the interflake one. The same is true for many other properties. Effects of MXene composition, including surface terminations, defects, flake size, and other characteristics on electronic, optical, magnetic, mechanical, and thermal properties need extensive studies. Finally, understanding the health and environmental safety/toxicity of MXenes with different transition metals and surface terminations is important for both, the manufacturing of MXenes and their applications.

Addressing the challenges listed above will require efforts of a large number of researchers representing different disciplines. However, the pay-off will be an enormously large family of 2D materials, with tunable properties that may impact numerous advanced technologies, from energy harvesting and storage to electronics, communication and medicine.

Declaration of competing interest

The authors declare that they have no known competing financial interests or personal relationships that could have appeared to influence the work reported in this paper. Materials Research Center, Ukraine, who sell equipment shown in Fig. 2, is directed by Dr. O. Gogotsi, related to Prof. Y. Gogotsi, but the author is not affiliated with the company.

Acknowledgements

The authors were supported by a U.S. National Science Foundation grant DMR-1740795.

References

- R. Mas-Balleste, C. Gomez-Navarro, J. Gomez-Herrero, F. Zamora, 2D materials: to graphene and beyond. Nanoscale 3 (1) (2011) 20–30.
- [2] K. Novoselov, A. Mishchenko, A. Carvalho, A.C. Neto, 2D materials and van der Waals heterostructures, Science 353 (6298) (2016) aac9439.
- [3] K.S. Novoselov, A.K. Geim, S.V. Morozov, D. Jiang, Y. Zhang, S.V. Dubonos, I. V. Grigorieva, A.A. Firsov, Electric field effect in atomically thin carbon films, Science 306 (5696) (2004) 666–669.
- [4] H. Oughaddou, H. Enriquez, M.R. Tchalala, H. Yildirim, A.J. Mayne, A. Bendounan, G. Dujardin, M.A. Ali, A. Kara, Silicene, a promising new 2D material, Prog. Surf. Sci. 90 (1) (2015) 46–83.

- [5] W.-g. Kim, S. Nair, Membranes from nanoporous 1D and 2D materials: a review of opportunities, developments, and challenges, Chem. Eng. Sci. 104 (2013) 908–924.
- [6] G. Eda, G. Fanchini, M. Chhowalla, Large-area ultrathin films of reduced graphene oxide as a transparent and flexible electronic material, Nat. Nanotechnol. 3 (5) (2008) 270.
- [7] C. Zhi, Y. Bando, C. Tang, H. Kuwahara, D. Golberg, Large-scale fabrication of boron nitride nanosheets and their utilization in polymeric composites with improved thermal and mechanical properties, Adv. Mater. 21 (28) (2009) 2889–2893.
- [8] B. Luo, G. Liu, L. Wang, Recent advances in 2D materials for photocatalysis, Nanoscale 8 (13) (2016) 6904–6920.
- [9] M. Naguib, M. Kurtoglu, V. Presser, J. Lu, J. Niu, M. Heon, L. Hultman, Y. Gogotsi, M.W. Barsoum, Two-dimensional nanocrystals produced by exfoliation of Ti₃AlC₂, Adv. Mater. 23 (37) (2011) 4248–4253.
- [10] M. Naguib, O. Mashtalir, J. Carle, V. Presser, J. Lu, L. Hultman, Y. Gogotsi, M. W. Barsoum, Two-dimensional transition metal carbides, ACS Nano 6 (2) (2012) 1322–1331.
- [11] Y. Gogotsi, Q. Huang, MXenes: two-dimensional building blocks for future materials and devices, ACS Nano 15 (2021) 5775–5780.
- [12] B. Anasori, Y. Gogotsi, 2D Metal Carbides and Nitrides (MXenes), Springer, Cham, 2019.
- [13] Y. Xia, T.S. Mathis, M.Q. Zhao, B. Anasori, A. Dang, Z. Zhou, H. Cho, Y. Gogotsi, S. Yang, Thickness-independent capacitance of vertically aligned liquid-crystalline MXenes, Nature 557 (7705) (2018) 409–412.
- [14] B. Anasori, M.R. Lukatskaya, Y. Gogotsi, 2D metal carbides and nitrides (MXenes) for energy storage, Nat. Rev. Mater. 2 (2) (2017) 1–17.
- [15] L. Wang, M. Han, C.E. Shuck, X. Wang, Y. Gogotsi, Adjustable electrochemical properties of solid-solution MXenes, Nano Energy 88 (2021), 106308.
- [16] A. VahidMohammadi, J. Rosen, Y. Gogotsi, The world of two-dimensional carbides and nitrides (MXenes), Science 372 (6547) (2021), eabf1581.
- [17] M.W. Barsoum, MAX Phases: Properties of Machinable Ternary Carbides and Nitrides, John Wiley & Sons, 2013.
- [18] M. Alhabeb, K. Maleski, B. Anasori, P. Lelyukh, L. Clark, S. Sin, Y. Gogotsi, Guidelines for synthesis and processing of 2D titanium carbide (Ti₃C₂T_x MXene), Chem. Mater. 29 (18) (2017) 7633–7644.
- [19] M. Ghidiu, M.R. Lukatskaya, M.Q. Zhao, Y. Gogotsi, M.W. Barsoum, Conductive two-dimensional titanium carbide 'clay' with high volumetric capacitance, Nature 516 (7529) (2014) 78–81.
- [20] J. Halim, M. Lukatskaya, K.M. Cook, C. Smith, S. May, J. Lu, L. Hultman, Y. Gogotsi, M.W. Barsoum, Transparent conductive two-dimensional titanium carbide thin filims, Chem. Mater. 26 (2014) 2374–2381.
- [21] C.E. Shuck, A. Sarycheva, M. Anayee, A. Levitt, Y. Zhu, S. Uzun, V. Balitskiy, V. Zahorodna, O. Gogotsi, Y. Gogotsi, Scalable synthesis of Ti₃C₂T_x MXene, Adv. Eng. Mater. 22 (3) (2020), 1901241.
- [22] C.E. Shuck, K. Ventura-Martinez, A. Goad, S. Uzun, M. Shekhirev, Y. Gogotsi, Safe synthesis of MAX and MXene: guidelines to reduce risk during synthesis, ACS Chemical Health & Safety 28 (5) (2021) 326–338.
- [23] C. Zhang, M.P. Kremer, A. Seral-Ascaso, S.-H. Park, N. McEvoy, B. Anasori, Y. Gogotsi, V. Nicolosi, Stamping of flexible, coplanar micro-supercapacitors using MXene inks, Adv. Funct. Mater. 28 (9) (2018), 1705506.
- [24] K. Maleski, V.N. Mochalin, Y. Gogotsi, Dispersions of two-dimensional titanium carbide MXene in organic solvents, Chem. Mater. 29 (4) (2017) 1632–1640.
- [25] F. Shahzad, M. Alhabeb, C.B. Hatter, B. Anasori, S.M. Hong, C.M. Koo, Y. Gogotsi, Electromagnetic interference shielding with 2D transition metal carbides (MXenes), Science 353 (6304) (2016) 1137–1140.
- [26] S.J. Kim, J. Choi, K. Maleski, K. Hantanasirisakul, H.-T. Jung, Y. Gogotsi, C.W. Ahn, Interfacial assembly of ultrathin, functional MXene films, ACS Appl. Mater. Interfaces 11 (35) (2019) 32320–32327.
- [27] T. Li, L. Yao, Q. Liu, J. Gu, R. Luo, J. Li, X. Yan, W. Wang, P. Liu, B. Chen, W. Zhang, W. Abbas, R. Naz, D. Zhang, Fluorine-free synthesis of high-purity Ti₃C₂T_x (T=OH, O) via alkali treatment, Angew. Chem. Int. Ed. 57 (21) (2018) 6115–6119.
- [28] V. Natu, M. Benchakar, C. Canaff, A. Habrioux, S. Célérier, M.W. Barsoum, A critical analysis of the X-ray photoelectron spectra of Ti₃C₂T_z MXenes, Matter 4 (2021) 1224–1251.
- [29] J. Xuan, Z. Wang, Y. Chen, D. Liang, L. Cheng, X. Yang, Z. Liu, R. Ma, T. Sasaki, F. Geng, Organic-base-driven intercalation and delamination for the production of functionalized titanium carbide nanosheets with superior photothermal therapeutic performance, Angew. Chem. 128 (47) (2016) 14789–14794.
- [30] H. Badr, T. El-Melegy, M. Carey, V. Natu, M.Q. Hassig, C. Johnson, Q. Qian, C.Y. Li, K. Kushnir, E.C. Ulloa, L.V. Titova, J. Martin, R.L. Grimm, R. Pai, V. Kalra, A. Karmakar, K. Liang, M. Naguib, O. Wilson, A.J.D. Magenau, K. Montazeri, Y. Zhu, H. Cheng, T. Torita, M. Koyanagi, A. Yanagimachi, T. Ouisse, M. Barbier, F. Wihlem, A. Rogalev, P. Persson, J. Rosen, Y.-J. Hu, M.W. Barsoum, Bottom-up, scalable synthesis of anatase nanofilament-based two-dimensional titanium carbooxide flakes, Mater. Today 54 (2022) 8–17.
- [31] S. Yang, P. Zhang, F. Wang, A.G. Ricciardulli, M.R. Lohe, P.W.M. Blom, X. Feng, Fluoride-free synthesis of two-dimensional titanium carbide (MXene) using a binary aqueous system, Angew. Chem. 130 (47) (2018) 15717–15721.
- [32] W. Sun, S.A. Shah, Y. Chen, Z. Tan, H. Gao, T. Habib, M. Radovic, M.J. Green, Electrochemical etching of Ti₂AlC to Ti₂CT_x (MXene) in low-concentration hydrochloric acid solution, J. Mater. Chem. 5 (41) (2017) 21663–21668.
- [33] M. Li, J. Lu, K. Luo, Y. Li, K. Chang, K. Chen, J. Zhou, J. Rosen, L. Hultman, P. Eklund, P.O.Å. Persson, S. Du, Z. Chai, Z. Huang, Q. Huang, Element replacement approach by reaction with Lewis acidic molten salts to synthesize

- nanolaminated MAX phases and MXenes, J. Am. Chem. Soc. 141 (11) (2019) 4730–4737.
- [34] V. Kamysbayev, A.S. Filatov, H. Hu, X. Rui, F. Lagunas, D. Wang, R.F. Klie, D. V. Talapin, Covalent surface modifications and superconductivity of two-dimensional metal carbide MXenes, Science 369 (6506) (2020) 979–983.
- [35] A. Jawaid, A. Hassan, G. Neher, D. Nepal, R. Pachter, W.J. Kennedy, S. Ramakrishnan, R.A. Vaia, Halogen etch of Ti₃AlC₂ MAX phase for MXene fabrication, ACS Nano 15 (2) (2021) 2771–2777.
- [36] M. Naguib, R.R. Unocic, B. Armstrong, J. Nanda, Large-scale delamination of multilayers transition metal carbides and carbonitrides "MXenes, Dalton Trans. 44 (2015) 9353.
- [37] O. Mashtalir, M. Lukatskaya, M.-Q. Zhao, M.W. Barsoum, Y. Gogotsi, Amineassisted delamination of Nb₂C MXene for Li-ion energy storage devices, Adv. Mater. 27 (2015) 3501–3506.
- [38] J. Halim, E.J. Moon, P. Eklund, J. Rosen, M.W. Barsoum, T. Ouisse, Variable range hopping and thermally activated transport in molybdenum-based MXenes, Phys. Rev. B 98 (2018), 104202.
- [39] V. Natu, R. Pai, O. Wilson, E. Gadasu, H. Badr, A. Magenau, V. Kalra, M. W. Barsoum, Effect of base/nucleophile treatment on interlayer ion intercalation, surface terminations and osmotic swelling of Ti₃C₂T_z MXene multilayers, Chem. Mater. 34 (2) (2022) 678–693.
- [40] P.Y. Bruice, Organic Chemistry, fourth ed., Pearson/Prentice Hall, Upper Saddle River, NJ, 2004.
- [41] O. Mashtalir, K.M. Cook, V.N. Mochalin, M. Crowe, M.W. Barsoum, Y. Gogotsi, Dye adsorption and decomposition on two dimensional titanium carbide in aqueous media, J. Mater. Chem. 2 (2014) 14334–14338.
- [42] A. VahidMohammadi, M. Mojtabavi, N.M. Caffrey, M. Wanunu, M. Beidaghi, Assembling 2D MXenes into highly stable pseudocapacitive electrodes with high power and energy densities, Adv. Mater. 31 (8) (2019), 1806931.
- [43] S. Huang, V.N. Mochalin, Understanding chemistry of two-dimensional transition metal carbides and carbonitrides (MXenes) with gas analysis, ACS Nano 14 (2020) 10251–10257.
- [44] S. Huang, V.N. Mochalin, Hydrolysis of 2D transition-metal carbides (MXenes) in colloidal solutions, Inorg. Chem. 58 (2019) 1958–1966.
- [45] T. Habib, X. Zhao, S.A. Shah, Y. Chen, W. Sun, H. An, J.L. Lutkenhaus, M. Radovic, M.J. Green, Oxidation stability of Ti₃C₂T_x MXene nanosheets in solvents and composite films, 2D Mater. Applic. 3 (2019) 8.
- [46] V. Natu, J.L. Hart, H. Chiang, M.L. Taheri, M.W. Barsoum, Edge capping of 2D-MXene sheets with polyanionic salts to mitigate oxidation in aqueous colloidal suspensions, Angew. Chem. 58 (2019) 12655–12660.
- [47] K. Matthews, T. Zhang, C.E. Shuck, A. VahidMohammadi, Y. Gogotsi, Guidelines for synthesis and processing of chemically stable two-dimensional V₂CT_x MXene, Chem. Mater. 34 (2) (2022) 499–509.
- [48] X. Wang, Z. Wang, J. Qiu, Stabilizing MXene by hydration chemistry in aqueous solution. Angew. Chem. Int. Ed. 60 (51) (2021) 26587–26591.
- [49] T.S. Mathis, K. Maleski, A. Goad, A. Sarycheva, M. Anayee, A.C. Foucher, K. Hantanasirisakul, C.E. Shuck, E.A. Stach, Y. Gogotsi, Modified MAX phase synthesis for environmentally stable and highly conductive Ti₃C₂ MXene, ACS Nano 15 (2021) 6420–6429.
- [50] J. Zhang, N. Kong, D. Hegh, K.A.S. Usman, G. Guan, S. Qin, I. Jurewicz, W. Yang, J. M. Razal, Freezing titanium carbide aqueous dispersions for ultra-long-term storage, ACS Appl. Mater. Interfaces 12 (2020) 34032–34040.
- [51] C.J. Zhang, S. Pinilla, N. McEvoy, C.P. Cullen, B. Anasori, E. Long, S.-H. Park, A. Seral-Ascaso, A. Shmeliov, D. Krishnan, C. Morant, X. Liu, G.S. Duesberg, Y. Gogotsi, V. Nicolosi, Oxidation stability of colloidal two-dimensional titanium carbides (MXenes), Chem. Mater. 29 (11) (2017) 4848–4856.
- [52] M.W. Barsoum, The MAX phases and their properties, in: R.R. Riedel, I.-W. Chen (Eds.), Ceramics Science and Technology, 2, Wiley-VCH, 2010.
- [53] T. Ouisse, M.W. Barsoum, Magnetotransport in the MAX phases and their 2D derivatives: MXenes, Mater. Res. Letts. 5 (2017) 365–378.
- [54] A. Gkountaras, Y. Kim, J. Coraux, V. Bouchiat, S. Lisi, M.W. Barsoum, T. Ouisse, Mechanical exfoliation of select MAX phases and Mo₄Ce₄Al₇C₃ single crystals to produce MAXenes, Small 16 (4) (2020), 1905784.
- [55] M.W. Barsoum, T. El-Raghy, Synthesis and characterization of a remarkable ceramic: Ti₃SiC₂, J. Am. Ceram. Soc. 79 (7) (1996) 1953–1956.
- [56] N. Medvedeva, D. Novikov, A. Ivanovsky, M. Kuznetsov, A. Freeman, Electronic properties of Ti₂SiC₂-based solid solutions, Phys. Rev. B 58 (1998) 16042–16050.
- [57] G. Hug, E. Fries, Full-potential electronic structure of Ti₂AlC & Ti₂AlN, Phys. Rev. B 65 (2002), 113104.
- [58] T. Ouisse, L. Shi, B.A. Piot, B. Hackens, V. Mauchamp, D. Chaussende, Magnetotransport properties of nearly-free electrons in two-dimensional hexagonal metals and application to the M_{n+1}AX_n phases, Phys. Rev. B 92 (2015), 045133.
- [59] T. Ouisse, D. Pinek, M.W. Barsoum, Modelling in-plane magneto-transport in Cr_2AlC , Ceram. Int. 45 (2019) 22956–22960.
- [60] A. Miranda, J. Halim, M.W. Barsoum, A. Lorke, Electronic properties of freestanding Ti₃C₂T_x MXene monolayers, Appl. Phys. Lett. 108 (2016), 033102.
- [61] A. Lipatov, M. Alhabeb, H. Lu, S. Zhao, M.J. Loes, N.S. Vorobeva, Y. Dall'Agnese, Y. Gao, A. Gruverman, Y. Gogotsi, A. Sinitskii, Electrical and elastic properties of individual single-layer Nb₄C₃T_x MXene flakes, Adv. Electron. Mater. 6 (4) (2020), 1901382.
- [62] A. Lipatov, M. Alhabeb, M.R. Lukatskaya, A. Boson, Y. Gogotsi, A. Sinitskii, Effect of synthesis on quality, electronic properties and environmental stability of individual monolayer Ti₃C₂ MXene flakes, Adv. Electron. Mater. 2 (2016), 1600255.
- [63] K. Hantanasirisakul, M. Alhabeb, A. Lipatov, K. Maleski, B. Anasori, P. Salles, C. Ieosakulrat, P. Pakawatpanurut, A. Sinitskii, S.J. May, Y. Gogotsi, Effects of

ARTICLE IN PRESS

M.W. Barsoum and Y. Gogotsi Ceramics International xxx (xxxx) xxx

- synthesis and processing on optoelectronic properties of titanium carbonitride MXene, Chem. Mater. 31 (8) (2019) 2941–2951.
- [64] A. Lipatov, A. Goad, M.J. Loes, N.S. Vorobeva, J. Abourahma, Y. Gogotsi, A. Sinitskii, High electrical conductivity and breakdown current density of individual monolayer Ti₃C₂T_x MXene flakes, Matter 4 (4) (2021) 1413–1427.
- [65] A.D. Dillon, M. Ghidiu, A. Krick, J. Griggs, S.J. May, Y. Gogotsi, M.W. Barsoum, A. T. Fafarman, Highly-conductive, optical-quality films from solution-processed 2D titanium carbide (MXene), Adv. Funct. Mater. 26 (2016) 4162–4168.
- [66] J. Halim, I. Persson, E.J. Moon, P. Kühne, V. Darakchieva, S.J. May, P.O.Å. Persson, P. Eklund, J. Rosen, M.W. Barsoum, Electronic and optical characterization of 2D Ti₂C and Nb₂C (MXene) thin films, J. Phys. Condens. Matter 31 (2019), 165301.
- [67] N.F. Mott, E.A. Davis, *Electronic Processes in Non-crystalline Materials* (Oxford Classic Texts in the Physical Sciences), second ed., 2012.
- [68] H. Kim, B. Anasori, Y. Gogotsi, H.N. Alshareef, Thermoelectric properties of twodimensional molybdenum-based MXenes, Chem. Mater. 29 (2017) 6472–6479.

- [69] J.L. Hart, K. Hantanasirisakul, A.C. Lang, B. Anasori, D. Pinto, Y. Pivak, J.T. v. Omme, S.J. May, Y. Gogotsi, M.L. Taheri, Control of MXenes' electronic properties through termination and intercalation, Nat. Commun. 10 (2019) 522.
- [70] B. Ánasori, C. Shi, E.J. Moon, Y. Xie, C. Voigt, E. Dooryhee, P.R.C. Kent, S.J. May, S. J.L. Billinge, M.W. Barsoum, Y. Gogotsi, Control of electronic properties of 2D carbides (MXenes) by manipulating their transition metal layers, Nanoscale Hor. 1 (2016) 227–234.
- [71] P.U. Jepsen, D.G. Cooke, M. Koch, Terahertz spectroscopy and imaging modern techniques and applications, Laser Photon. Rev. 5 (1) (2011) 124–166.
- [72] G. Li, V. Natu, T. Shi, M.W. Barsoum, L.V. Titova, Two-dimensional MXenes Mo₂Ti₂C₃T_z and Mo₂TiC₂T_z: microscopic conductivity and dynamics of photoexcited carriers, ACS Appl. Energy Mater. 3 (2) (2020) 1530–1539.
- [73] G. Li, K. Kushnir, Y. Dong, S. Chertopalov, A.M. Rao, V.N. Mochalin, R. Podila, L. V. Titova, Equilibrium and non-equilibrium free carrier dynamics in 2D Ti₃C₂T_x MXenes: THz spectroscopy study, 2D Mater. 5 (3) (2018), 035043.
- [74] K. Hantanasirisakul, Y. Gogotsi, Electronic and optical properties of 2D transition metal carbides and nitrides (MXenes), Adv. Mater. 30 (52) (2018), 1804779.